Dynamic Nanoindentation Analysis using Generalized Maxwell Model for Viscoelastic Materials Characterization

Philip A. Yuya* and Nimitt G. Patel**

* Mechanical and Aeronautical Engineering Department, Clarkson University, Potsdam, NY 13699
pyuya@clarkson.edu
** Materials Science and Engineering Program, Clarkson University, Potsdam, NY 13699
patelng@clarkson.edu

ABSTRACT

A model is implemented that captures the dynamic nanoindentation response of a viscoelastic material. Indenter tip-sample contact forces are modeled using a generalized Maxwell model**.** Further, this model is used to derive empirical formulas to fit experimental dynamic nanoindentation data. Using natural latex rubber as a test sample, dynamic nanoindentation experiments were performed with a 108 μm diamond cono-spherical tip at ambient conditions. The results were analyzed using conventional Voigt model and contrasted with analysis done using the Maxwell-standard linear solid model. The results show that conventional Voigt model overestimates the storage modulus of the latex sample by ~ 37 percent. The analysis will prove useful for quantitative nanoindentation property measurements of viscoelastic materials such as rubbery polymers and soft biological materials.

Keywords: Viscoelasticity, Maxwell Model, Dynamic Nanoindentation, Standard Linear Solid

1. INTRODUCTION

Nanoindentation has become a very useful tool for materials properties characterization at nanoscale. The technique relies on the local deformation induced on a material's surface with an indenter of known properties under the application of a given load. The technique has been used to investigate mechanical properties of thin films [1-4], hard mineralized tissues and glassy polymers [5], and more recently, soft biological tissues [6]. For most elastic-plastic materials, such as metals and ceramics, the Oliver and Pharr [1] method has been used to accurately determine elastic modulus and hardness. For viscoelastic materials that exhibit a time-dependent stress-strain response, the analysis of nanoindentation data by this method usually leads to large errors.

Different approaches such as quasi-static, ramp and hold creep [7] and dynamic nanoindentation have been used to characterize properties for soft materials. While quasi-static nanoindentation can yield accurate information about materials' elastic properties, development is needed to characterize viscoelastic materials with dynamic nanoindentation [8]. Dynamic nanoindentation involves the superposition of a small sinusoidal load onto a DC quasi-static load and measurement of the steady-state vibrational response of the system using a lock-in amplifier [9]. The Kelvin-Voigt (two-parameter) solid has been used as the conventional model for the tip-sample forces for viscoelastic contact. In the two-parameter model, sample stiffness is represented with a spring of stiffness k and the damping represented by a dash-pot with damping c [10,11]. This model captures the essence of viscoelastic behavior and is simple to implement; however, the two-parameter model oversimplifies the response of most viscoelastic materials. It is limited to modeling material response at a single frequency, because it only incorporates a single relaxation time. Furthermore, it does not account for instantaneous elasticity and therefore underestimates contact forces [12]. Accurate characterization of material properties with a nanoindenter is critically dependent on the ability to both correctly model the frequency response of the test equipment in contact with the material and the correct choice of indenter tip geometry.

In this work, the indenter tip-sample contact forces are modeled using a generalized Maxwell model. This model is used to derive empirical formulas to fit the experimental dynamic nanoindentation data to determine the material parameters. Using this model, the storage and loss indentation moduli are calculated by applying the fit parameters within the formulas. Important features of the experimental method are discussed and results of natural rubber latex are presented. Additionally, the results based on Voigt model analysis are compared with the results analyzed with Maxwell-standard linear solid (M-SLS).

2. THEORETICAL MODEL

A viscoelastic model commonly used to represent the response of real materials is the Wiechert (generalized Maxwell model) model [13]. In this model, springs represent elastic response while dashpots account for dissipation in the material. A free stiffness, k_∞ represents the long-time behavior exhibited by some viscoelastic materials. It provides equilibrium or rubbery stiffness that remains after the stresses in the Maxwell arm have relaxed as the dashpot extends.

During dynamic nanoindentation, a harmonic forcing function of the form $F(t) = F_0 e^{i(\omega t+\phi)}$ would result in harmonic displacement expressed by $x = X_0 e^{i\omega t}$ here, X_0 is the amplitude of the displacement at the same driving frequency ω which lags the oscillation of the applied force of amplitude F_0 by a phase angle ϕ. The steady-state harmonic response then becomes,

$$F_{\text{Maxwell}} = X_0 e^{i\omega t}\left[k_\infty + \sum_{j=1}^{M} \frac{i\omega c_j k_j}{(i\omega c_j + k_j)}\right], \quad (1)$$

here, F_{Maxwell} is the contribution of the resisting force due to the generalized Maxwell model consisting of spring and damping constants. F_{Maxwell} is complex with real and imaginary parts. The real part represents the storage stiffness (k_{storage}), while the imaginary part is the loss stiffness (k_{loss}).

A representation of instrument-sample interaction during dynamic testing of a viscoelastic material using generalized maxwell model is shown in figure 1. The differential equation of motion of the system is given by

$$F(t) = m\ddot{x}(t) + k_i x(t) + c_i \dot{x}(t) + F_{\text{Maxwell}} \quad (2)$$

where, k_i, c_i, and m represent the instrument stiffness, damping and mass, respectively and F_{Maxwell} is the contribution to the resisting force caused by the Maxwell model.

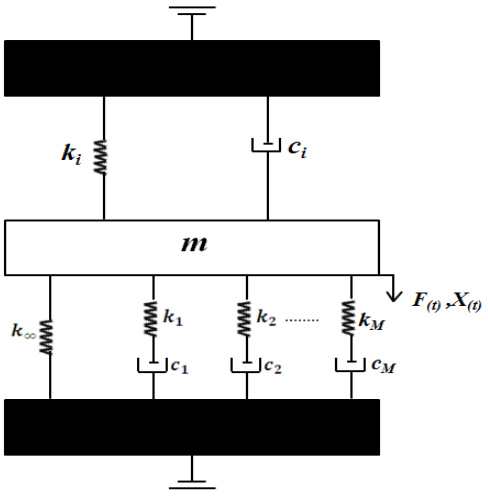

Figure 1. Mechanical model used for nanoindentation system with a generalized Maxwell solid to account for material response.

The dynamic compliance function obtained from solving the differential equation of motion for the system is represented as

$$\left|\frac{X_0}{F_0}\right| = \left\{\left(k_i + k_{\text{storage}} - m\omega^2\right)^2 + \omega^2(C_i + k_{\text{loss}})^2\right\}^{-\frac{1}{2}} \quad (3)$$

and the phase shift between the applied force amplitude and displacement amplitude is given by

$$\tan(\phi) = -\frac{\omega(c_i + k_{\text{loss}})}{\left(k_i + k_{\text{storage}} - m\omega^2\right)}. \quad (4)$$

Equations (3) and (4) depend on both the indenter parameters and material constants. Indenter constants are determined from free (tip out of contact) dynamic nanoindentation data by setting $k_{\text{storage}} = k_{\text{loss}} = 0$ in Eqs. (3) and (4) during the calibration process. Material constants are then determined by fitting Eqs. (3) and (4) to contact frequency spectra data obtained experimentally using known values of k_i, c_i, and m determined from calibration tests.

In the limit of linear viscoelasticity, the elastic–viscoelastic correspondence principle is used to relate the dynamic stiffness and damping of the contact to modulus values. By making use of Hertzian [14] contact mechanics model, the storage indentation modulus is expressed as

$$M' = \frac{E'}{1-\nu^2} = \frac{k_{\text{storage}}}{2}\sqrt{\frac{\pi}{A_c}}, \quad (5)$$

and the loss indentation modulus is given by

$$M'' = \frac{E''}{1-\nu^2} = \frac{k_{\text{loss}}}{2}\sqrt{\frac{\pi}{A_c}}, \quad (6)$$

where, ν is the Poisson's ratio, A_c is the contact area between the tip and sample, E' and E'' are the storage and loss moduli, respectively.

A useful measure of the relative contributions of the storage and loss moduli to the mechanical response of a material is given by the loss factor defined as

$$\tan(\delta) = \frac{k_{\text{loss}}}{k_{\text{storage}}} \quad (7)$$

which is a measure of damping in a linear viscoelastic material. Tan (δ) > 1 indicates a predominantly viscous or fluid-like behavior whereas tan (δ) < 1 indicates a predominantly solid-like response. The loss factor is anadvantageous parameter in nanoindentation analysis, because errors associated with contact area are eliminated. Considering tip-sample contact as a M-SLS (three-parameter model), contact storage stiffness and loss stiffness are derived from Eq. (1) respectively as,

$$k_{\text{storage}} = \left|\frac{F_0}{X_0}\right| cos(\phi) = \frac{k_\infty k_1^2 + \omega^2(k_\infty c_1^2 + k_1 c_1^2)}{(k_1^2 + \omega^2 c_1^2)}, \quad (8)$$

$$k_{\text{loss}} = \left|\frac{F_0}{X_0}\right| sin(\phi) = \frac{\omega(k_1^2 c_1)}{(k_1^2 + \omega^2 c_1^2)}. \quad (9)$$

These expressions are substituted in equations (3) and (4) which is then used to fit experimental data allowing the determination of the viscoelastic parameters.

3. MATERIALS AND METHODS

A commercial disposable exam glove made of natural rubber latex with thickness of 110 µm (Cranberry USA Inc., American Canyon, CA, USA) was cut and glued onto magnetic sample holder disc. The tests were performed at room temperature using a TI 950 TriboIndenter, (Hysitron Inc., Minneapolis, MN). All tests were performed using a large cono-spherical tip (radius ~108 µm) in order to maintain purely elastic tip-sample interractions [6,8,14].

A dynamic nanoindentation technique was used to determine the viscoelastic properties of latex rubber. The tip was loaded at a rate of 50 µN/s and held at a maximum peak force of 500 µN resulting in an average maximum contact depth of 1400 nm (less than 10 percent of the sample thickness). During the hold period, a small sinusoidal force was superimposed onto the quasi-static load causing the tip to oscillate about its equilibrium indentation depth. The dynamic force amplitude used was 5 µN, which resulted in displacement amplitudes of approxiamtely 15-30 nm. During the holding period, the frequency of the dynamic load was adjusted incrementally between 10-100 Hz and 110-200 Hz. In both cases,15 equally-spaced steps were used to ensure relatively short test times. For soft materials, longer test times can skew results due to non-constant drift rates and can result in an artificial increase in the contact depth due to material creep. At each frequency, a lock-in amplifier measured the displacement amplitude and phase lag of the displacement response relative to the input forcing signal.

4. RESULTS AND DISCUSSION

An example of contact spectra (dynamic compliance and phase) are shown in Figure 2. Material response and parameters are determined by subtracting the instrument's contributions from the total measured response. The results were analyzed using two models: (1) the conventional Voigt model and (2) M-SLS. A least-square nonlinear fit to Eqs. (3) and (4) was performed on the experimental data (compliance and phase) to obtain the model constants k_∞, k_1 and c_1 for the M-SLS analysis. A similar approach has been used in the contact resonance force microscopy (CR-FM) technique for viscoelastic properties measurements [11]. The M-SLS fits are indicated in Figure 2 with solid red line. For the Voigt model analysis, the fit was performed using equations presented by Asif *et al.* [9]. Fits using the Voigt model are also shown in Figure 2 with blue dots. Overall good agreement between both models and experimental data is apparent. In both cases, the predicted response matches the experimental results.

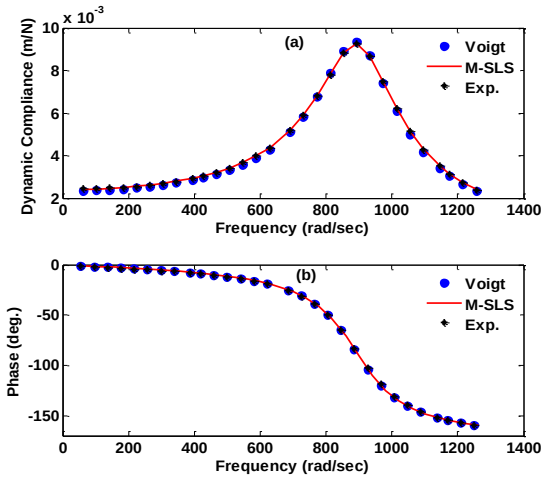

Figure 2. Example of frequency response of the indenter tip in contact with latex showing, (a) dynamic compliance and (b) phase shift. Experimental results are shown using diamond symbol with the Maxwell-SLS model fit shown as a solid red line and Voigt model as blue dots.

The material stiffness values were calculated from the material constants obtained from curve fitting. Equations (8) and (9) were solved to determine the storage and loss stiffness, respectively, for M-SLS model. For the Voigt model, the storage stiffness is represented by the stiffness of the sample (k_s) while the loss stiffness is given by the product of the frequency with the damping constant value (ωc_s). Indentation moduli were calculated from the stiffness values using Eqs. (5) and (6). For a spherical tip of tip-radius *R*, the contact area is given by, $A_c = -\pi h_c^2 + 2\pi R h_c$, where h_c is the contact depth.

Illustrating data for the mean of 8 measurements, a direct comparison of moduli values as a function of frequency for the two models is shown in Fig. 3. The hollow circles represent the modulus values obtained using Voigt model while the filled dots are values obtained using M-SLS model. The storage modulus values obtained using Voigt model are higher than those analyzed by M-SLS model. Both models give fairly constant storage modulus values as a function of the excitation frequency. Loss modulus values show an increase for both models as the excitation frequency is increased (Figure 3). At low frequencies, both models give similar loss modulus values, however, as the frequency is increased, loss modulus values obtained by Voigt model are slightly higher than those obtained by M-SLS. The increase in loss modulus with excitation frequency indicates an enhancement of the sample damping capacity at higher frequencies.

At an excitation frequency of 507 rad/s, analysis using Voigt model gives an indentation storage modulus value of 1.77 MPa, while similar analysis using M-SLS gives a value of 1.29 MPa for storage modulus. At this frequency,

Voigt model overestimates the indentation modulus value for this particular sample (latex) by ~37% compared to analysis by M-SLS model. Theoretically, as the excitation frequency approaches zero (quasi-static), the storage modulus should approach the elastic modulus values of the sample. Figure 4 shows a plot of the loss factor as a function of frequency. Both models show an increase in the loss factor value with increasing excitation frequency. The increase can be associated with localized softening of the sample due to greater amount of energy dissipated in the near surface region [5].

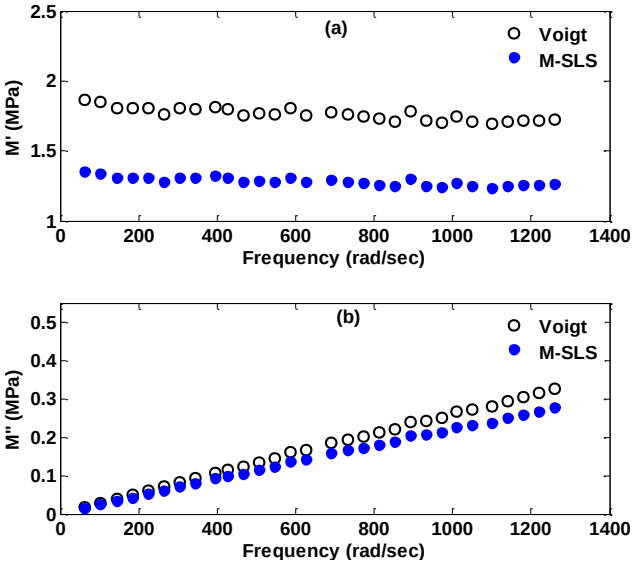

Figure 3. The storage and loss indentation moduli for latex as a function of frequency when modeling the tip-sample forces as a M-SLS and as a Voigt solid.

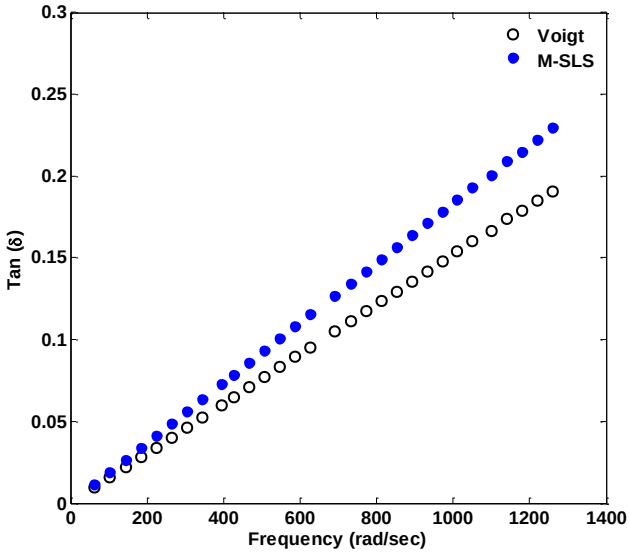

Figure 4. Loss factor of latex as a function of frequency when modeling the tip-sample forces as a M-SLS and as a Voigt solid.

5. SUMMARY AND CONCLUSION

A generalized Maxwell model has been implemented for dynamic nanoindentation analysis to accurately capture the true response of viscoelastic materials. To demonstrate the accuracy of the model, a simple case of the generalized model (Maxwell-standard linear solid) was used to analyze experimental results on latex and the results compared with those analyzed using conventional Voigt model. The results show that analysis based on a Kelvin-Voigt two parameter model, which works well for most glassy polymers, overestimates the material stiffness for latex rubber, resulting in higher values for the storage modulus. Therefore, a more refined model incorporating more elements should be used to accurately analyze dynamic nanoindentation data for such materials. The measured frequency response is a combination of both the indenter parameters and tip-sample contact forces; therefore, proper systems calibration is necessary to ensure accurate measurements. It has also been shown that model constants necessary for determining material stiffness values can be obtained by fitting a frequency response function to the data obtained experimentally. This work shows that for rubbery polymers, analysis of dynamic nanoindentation data using two-parameter Kelvin-Voigt model overestimates the.

REFERENCES

[1] G. M. Pharr and W. C. Oliver, MRS Bulletin, 17, 7, pp. 28-33, (1992)

[2] M. V. Swain and J. Menčík, Thin Solid Films, 253, 1–2, pp. 204-211, (1994).

[3] X. Chen and J. J. Vlassak, J. Mater. Res., 16, 10, pp. 2974-2982, (2001).

[4] Z. Shan, S. K. Sitaraman, Thin Solid Films 437, pp. 176–181 (2003).

[5] A. Chakravartula and K. Komvopoulos, Applied Physics Letter, 88, pp. 221908-1–221908-3, (2006)

[6] D. M. Ebenstein and L. A. Pruitt, J. Biomed. Mater. Res. A 69A (2), pp. 222-232 (2004)

[7] A. K. Bembey, M. L. Oyen, A. J. Bushby and A. Boyde, Philosphical Magazine, 86 (33-35), pp. 5691-5703 (2006)

[8] M. L. Oyen, Philosophical Magazine, 86 (33-35), pp. 5625-5641, (2006)

[9] S. Asif, K. J. Wahl, R.J. Colton, Review of Scientific Instruments, 70, 5, pp. 2408-2413, (1999)

[10] E. G. Herbert, W. C. Oliver, and G. M. Pharr, J. Phys. D: Appl. Phys. 41, pp. 1-9, (2008).

[11] P. A. Yuya, D. C. Hurley, and J. A. Turner, J. Appl. Phys. 104, pp. 074916-1 - 074916-7 (2008)

[12] W. J. Wright, A. R. Maloney and W. D. Nix, Int. J. Surface Sci. and Eng., 1, 2-3, pp. 274-292 (2007)

[13] R. M. Christensen, Theory of viscoelasticity, 2nd Edition. Dover, New York, (2003)

[14] K. L. Johnson, Contact mechanics, Cambridge University Press., Cambridge (1985)